AN ANALYSIS OF THE MEMBRANE POTENTIAL ALONG A CLAMPED SQUID AXON

KENNETH S. COLE
From the National Institutes of Health, Bethesda

ABSTRACT A partially depolarized squid axon membrane is assumed to have a quasi-steady state negative resistance, the membrane potential is clamped at one point, and a distribution of potential along the axon is obtained from the cable equation. Nominal experimental values of -2 ohm cm^2 for the membrane and 6 ohm cm^2 for the internal and external current electrodes and the axoplasm and sea water between them are used for illustration. The potential and current may be uniform for an axon and electrode length less than 1.2 mm. For a long axon the potential varies as the cosine of the distance within 0.8 mm of the control point. Beyond this the potential variation is exponential and the entire pattern is about 5 mm long. The average current density out to 0.3 mm from the control point is within 10 per cent of the potential clamp value. These distributions are stable for control amplifications of about unity and more.

INTRODUCTION

The concept of control of the electrical potential difference across an excitable membrane was developed and applied to the squid axon in the hope of measuring the ionic membrane current without either the spatial variations of a propagating impulse or the temporal instability which produced all-or-none excitation (Cole, 1949). Although this hope was more than realized in the original measurements, the extensions and analyses of them made by Hodgkin, Huxley, and Katz (HHK, 1952) and Hodgkin and Huxley (HH, 1952*a, b, c, d*) were so important as to open a new era of electrophysiology. But this progress brought with it an increased weight of responsibility for the validity of the experimental data that was neither anticipated nor even recognized for some time.

In such voltage clamp experiments the membrane potential of the axon is changed and maintained, on command, by electronic control of the current flow between long internal and external electrodes. The membrane current has been measured over a more or less restricted length of axon in all the work while the length of the potential electrode has been reduced at each stage of development. In our experimental work the potential measurement has been restricted, as described by Cole and Moore

(CM, 1960), to a small region called the control point and the present analysis is developed for this arrangement.

It has been found (CM) that the membrane potential of most squid axons could be adequately controlled over a considerable length with rather low resistance, or good, current electrodes. But with mediocre and bad electrodes or with the most powerful and interesting axons the control might become entirely inadequate at a short distance from the control point (Taylor, Moore, and Cole (TMC, 1960)). The distribution of membrane potential in the neighborhood of the point from which it is controlled is thus quite important in the understanding, design, and interpretation of voltage clamp experiments. The experimental results have so far been too varied and complicated for a satisfactory empirical description, and although they can neither guide nor indicate the validity of a theoretical approach, the only recourse at present is to analysis.

The most complete and satisfactory answer to this problem would be in the form of solutions of the cable and Hodgkin and Huxley equations for the membrane potential and current as functions of both time and distance along the axon. There is no apparent hope of solutions in analytical form for anything more complicated than the perfect voltage clamp. Although the problem is well within the power and capacity of present day digital computers, the cost in time, effort, and money has prevented more than a cautious start in this important direction. Consequently far more modest and directly understandable approaches have been made.

The steady state equations and the solutions for positive membrane conductances have been evolved from cable theory and the space constants computed (CM, TMC) to show the short lengths involved with low resistance current electrodes. There are also many unpublished investigations of approximations to various experimental conditions involving "resting" and "active" positive membrane conductances, mostly by Dr. R. E. Taylor along with some resistor network analog solutions by Dr. J. W. Moore. In most of these the conductances have been taken from the Hodgkin and Huxley equations or from more recent data. The resting conductances have been linear approximations to the low conductance found for steady hyperpolarization and to the high conductance for steady depolarization at zero and positive membrane potentials. The active positive conductance has been taken as a linear approximation to the early peak currents for depolarizations to -10 mv and more positive potentials.

There were, however, no more than superficial attempts to analyze the variations of the membrane potential and current in the vicinity of the control point for the all important range of potentials between -40 mv and -20 mv in which the peak inward membrane current increases rapidly. In this paper at least initial steps are taken to fill in this gap in an understanding of the technical requirements for an adequate implementation of the voltage clamp concept. Even a highly simplified and elementary approach to the general problem can be rather involved, but such results

have been found a very useful guide towards obtaining adequate control of the membrane potential.

The first and natural step was to approximate the early peak inward currents after depolarizations to potentials between −40 mv and −20 mv by a steady state negative conductance, as shown in Fig. 1. An alternative has been to similarly approximate the "isochronal" curves for the currents at a constant time after the application of potential change into this range. The steepest slopes—the maximum absolute values of the negative conductance—in each case have usually been nearly

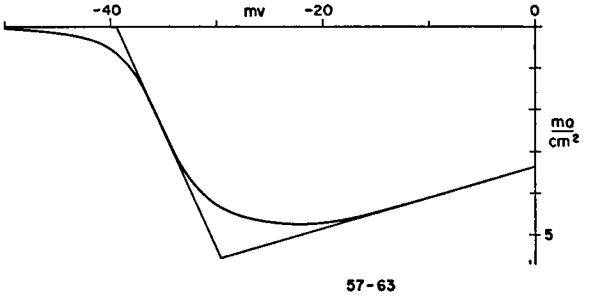

FIGURE 1 Peak inward current after depolarizations from −65 mv to potentials given as abscissae, heavy curve, and as approximated for analysis by three linear segments.

equal to each other. Stated in resistance terms the Hodgkin and Huxley membrane is about −25 ohm cm², normally, and about −13 ohm cm², when previously hyperpolarized by 20 mv. In a more recent set of experiments the resistances ranged from −1.6 ohm cm² to −8 ohm cm² with an average of −3.4 ohm cm², and a value of −2 ohm cm² has been taken to represent the most powerful axons in this "excitation" or "excited" range.

Such values of negative resistance or conductance have proved a very useful guide to the understanding of instability and the setting of requirements for the resistance of the current electrodes (CM, TMC). They have, however, been used with very considerable misgivings. They are not steady state characteristics and there was no reason to do more than hope that they were even in a quasi-steady state category. Furthermore, there was no real basis to expect that stability or instability was any more than remotely related to this value.

It was thus necessary to investigate the behavior of a patch of membrane, over which the potential and current were uniform, with some series resistance. By analog computation Moore and FitzHugh found a gross instability after the application of a constant depolarization to the Hodgkin and Huxley membrane and 50 ohm cm² in series. By analog computations also, Taylor and FitzHugh showed that although a single hyperpolarized Hodgkin and Huxley patch was easily controlled by feedback through a 10 ohm cm² resistance, an identical parallel, but uncon-

trolled, patch and resistance would show an occasional marked distortion in the time course of the current (TMC).

This problem has been investigated more thoroughly by Chandler (1961) with detailed digital calculations of the critical series resistance at the boundary between stability and instability for a Hodgkin and Huxley membrane initially hyperpolarized by 20 mv. It was found that the minimum value of this resistance, 12 ohm cm^2, was reached at nearly the same time and potential and was within 10 per cent of the negative resistances obtained from both the peak and the isochronal current *versus* potential relationships. There is thus a basis to believe that such a membrane will be stable for a smaller series resistance and to fear instability for a larger value. It is then possible to make the next step with rather more confidence and so to assume that for the more recent axons an estimate of -2 ohm cm^2 may be used as a quasi–steady state value to describe and predict the performance of such an axon. Although the correspondence may be somewhat less satisfactory it has been convenient for some purposes to further assume that the entire peak or isochronal currents as a function of potential represent the steady state characteristic of the membrane.

ASSUMPTIONS AND APPROXIMATIONS

The axon and electrodes are assumed to be the same everywhere in both geometry and electrical properties. The electrodes, axoplasm, and sea water are represented by pure, ohmic resistances. The ionic current through the membrane is an approximation to the early component of the voltage clamp current. It is, however, considered to be in a steady state. The value at each potential is at the time of the peak value as given by recent experiments and as suggested by the calculations of the stability of the hyperpolarized HH axon and the accompanying anomalous reactance is not otherwise taken into account. The ionic path is considered to be in shunt with a static membrane capacity of 1 $\mu f/cm^2$. The model for an axon with an internal, axial electrode and the corresponding cable equations (CM, Fig. 7 and equation (3); TMC, Fig. 17 and equation (1)) have been simplified as before when it was found that the external longitudinal variations of potential were negligible (TMC, equation (9)).

At this stage of approximation the problem is considerably less formidable and the straightforward solution given by equation (2) seems reasonably possible for numerical or analog calculation. Also an expression for the membrane current-potential characteristic might be found that would permit an analytical solution. Nevertheless the problem has been further idealized by approximating the assumed steady state characterisic by the three linear segments as shown in Figs. 1 and 3.

The three segments I, II, III are taken to have steady state or "slope" resistances of 1000 ohm cm^2, -2 ohm cm^2, and 6 ohm cm^2 and may be called the resting, excited, and active regions respectively. The corresponding conductances for a 480

μ axon are then about $1.4 \cdot 10^{-5}$ mho/mm, $-7 \cdot 10^{-3}$ mho/mm, and $2.3 \cdot 10^{-3}$ mho/mm respectively.[1] The longitudinal resistance of the axoplasm is taken to be $1.5 \cdot 10^{4}$ ohm/cm and the corresponding conductance is $7 \cdot 10^{-4}$ mho mm. The electrodes, axoplasm, and sea water are given the nominal resistance value of 6 ohms for a cm^2 of axon membrane corresponding to about $2.3 \cdot 10^{-3}$ mho/mm.

Further, for most present purposes and by comparison with these other conductances, the effect of the resting membrane is negligible and is assumed to be zero. Similarly, region III will be found to contribute more to confusion than to clarity and it will not be considered in any detail.

ANALYSIS

The usual procedures and the assumptions stated give the cable equation in a convenient form for the analysis as

$$\frac{\partial^2 V}{\partial x^2} = (i_3 - i_1)/g_2 \tag{1}$$

As shown in Fig. 2, V is the membrane potential relative to the outside which is at zero potential, i_3 and i_1 are the outward radial current densities in the membrane and

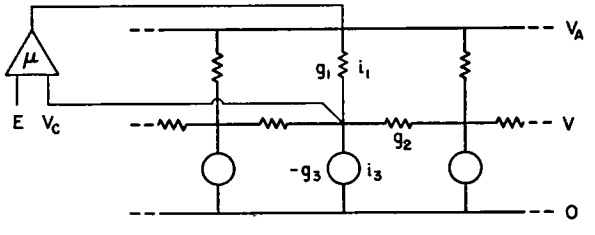

FIGURE 2 Equivalent circuit for an analysis of the squid axon membrane potential under point control. V is the potential of the membrane with a negative conductance $-g_3$ and a current density i_3. g_2 is the longitudinal conductance of the axoplasm. The radial conductance, g_1, includes the contributions of the axial and external electrodes, the axoplasm, and sea water. The control amplifier, μ, produces the potential of the axial electrode, V_A, to bring the potential of the control point, V_C, close to the command, E.

axoplasm, respectively, for a millimeter length of axon, and g_2 is the internal longitudinal conductance of the axoplasm in mho mm.

This equation may be solved formally in steady state, by integration with the factor $2\ dV/dx$

$$2 \int \frac{d^2 V}{dx^2} \cdot \frac{dV}{dx} \cdot dx = \frac{2}{g_2} \int (i_3 - i_1) \cdot \frac{dV}{dx} \cdot dx + K$$

[1] The millimeter is the most convenient unit for the axon lengths involved.

or

$$\left(\frac{dV}{dx}\right)^2 = \frac{2}{g_2}\int (i_3 - i_1)\, dV + K$$

and for $dV/dx = 0$, $V = V_A$, and $i_3 = i_1$ at $x = \infty$

$$\frac{dV}{dx} = \sqrt{\frac{2}{g_2}\int_{V_A}^{V} (i_3 - i_1)\, dV}. \tag{2}$$

When $i_3 - i_1$ is given analytically or numerically a second integration gives $V(x)$.

For an electrolyte and electrode conductance of g_1 mho/mm and an axial electrode or "wire" potential V_A

$$i_1 = g_1(V_A - V) \tag{3}$$

while in the steady state we have first assumed

$$i_3 = g_3(V_B - V) \tag{4}$$

in which $g_3 > 0$ is the numerical value of the negative conductance in mho/mm for the linear approximation to region II of the quasi-steady state characteristic for $V > V_B$, the "break point" between regions I and II. Then in steady state

$$\frac{d^2V}{dx^2} + \frac{g_3 - g_1}{g_2} V = \frac{g_3 V_B - g_1 V_A}{g_2}$$

For a symmetrical solution about $x = 0$ in which $dV/dx = 0$ at $x = 0$ and $\pm \infty$, we have for $x > 0$ in regions I or III

$$V = A \exp(-\alpha x) + B \tag{5}$$

with $\alpha^2 = (g_1 + g_3)/g_2$ using the value of g_3 for the region and

$$V = C \cos \omega x + D \tag{6}$$

with $\omega^2 = (g_3 - g_1)/g_2$ for V in region II and $g_3 > g_1 > 0$.

Confining our attention to regions I and II as shown in Fig. 4, the evaluation of the constants A, B, C, D, with the added conditions that V and dV/dx are continuous at V_B, and when needed that

$$\int_0^\infty (i_3 - i_1)\, dx = 0$$

gives the solution

$$V = V_A - (V_A - V_B) \exp[-\alpha(x - x_B)], \qquad V \leq V_B, \tag{7}$$

$$V = \bar{V} - \frac{\sqrt{g_1 g_3}}{g_3 - g_1}(V_A - V_B) \cos \omega x, \qquad V \geq V_B, \tag{8}$$

where

$$\bar{V} = \frac{g_3 V_B - g_1 V_A}{g_3 - g_1}$$

is the potential at which $d^2V/dx^2 = 0$ and the point x_B, the boundary between regions I and II where $V = V_B$, is given by

$$\cos \omega x_B = -\sqrt{g_1/g_3}.$$

The most important present conclusion to be reached is the variation of the membrane current density in the neighborhood of the central point. From equations (3), (4), and (8) the difference of the current densities, i_C and i, at the center and at a distance x from it is

$$\frac{i_C - i}{i_C} = \frac{\sqrt{g_3/g_1}}{1 + \sqrt{g_3/g_1}} (1 - \cos \omega x)$$

A difference of 20 per cent from the central point current then appears at 0.3 mm on each side of it as mentioned by CM and shown in Fig. 5. This corresponds to an error of less than 10 per cent in the average current density measured over this length but any separation of an external current measuring electrode, 0.6 mm long, away from the membrane will again increase the error of the average. On the other hand the distribution will probably give considerably less than 5 per cent error in the current density measured by differential electrodes with a resolution of 0.3 mm (*cf.* TMC).

PHASE PLANE SOLUTIONS

It has been found relatively simple and particularly illuminating to adapt the topological techniques widely used in non-linear mechanics (Minorsky, 1947) to the analysis of equation (1). The steady state solutions are here represented as lines on a phase plane with the coordinate axes V and $y = dV/dx$ rather than the more usual one on which $y = dV/dt$.

With

$$\frac{d^2V}{dx^2} = \frac{dy}{dx} = y \frac{dy}{dV}$$

equation (1) becomes

$$\frac{dy}{dV} = \frac{(i_3 - i_1)/g_2}{y} \tag{9}$$

and, with i_3 and i_1 known functions of V, lines called trajectories can be drawn with this slope at each point to represent solutions of the original equation. Solutions for non-linear functions, such as shown in Fig. 1, may be obtained in this way. The linear segment approximation gives solutions on this plane in which exp αx is a straight line, cos ωx an ellipse, and cosh αx a hyperbola, and the considerable confusing detail of an analytical solution is not apparent.

Some solutions of equation (9) are given for one value of V_A in Figs. 3 and 4. Here the upper half plane is for $x < 0$ and the lower half for $x > 0$. The solution

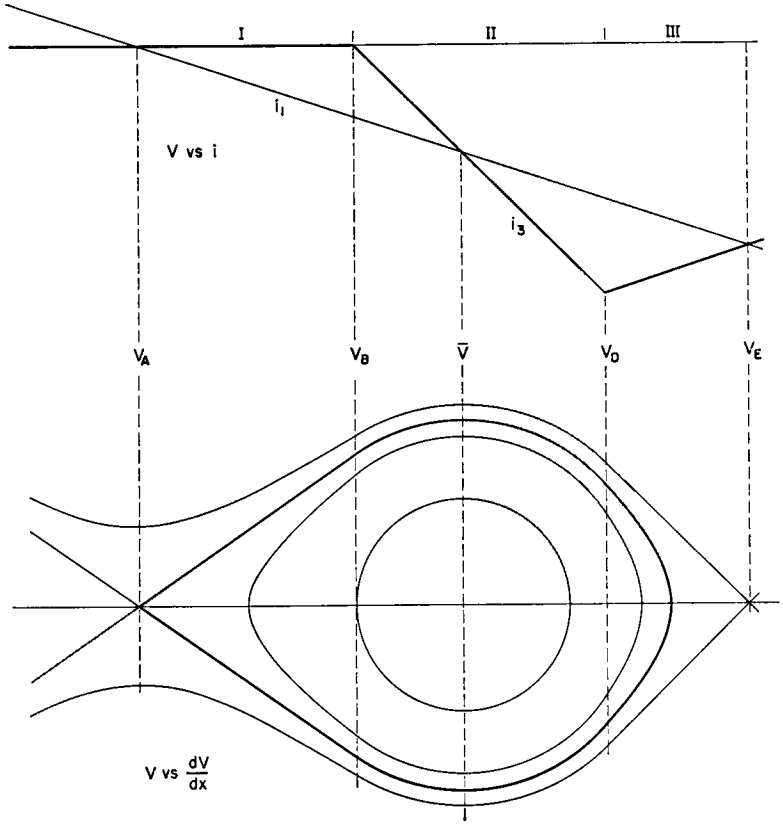

FIGURE 3 *V versus i* characteristics for membrane current, i_3, with linear regions I, II, III, and for series current, i_1, with axial electrode potential V_A (upper). Steady state solutions of cable equation on phase plane, *V versus dV/dx*, for several boundary conditions (lower).

corresponding to equation (5) and (6) is the heavier trajectory of Fig. 4. As can be shown directly from equation (9) it is the two straight lines in region I, two circular arcs (obtained by proper scaling) in region II, and also a hyperbola for region III in Fig. 3. The other trajectories, hyperbolas in regions I and III and circles in region II, satisfy other boundary conditions.

In particular in Fig. 3 it is seen that the exponential solutions to the point (V_B, 0) continue to diverge with indefinitely increasing y as V becomes less than V_A and thus are not found to represent a plausible physical situation. On the other hand beyond a definite more negative value for V_A the situation is reversed and a closed finite solution is found terminating for a value of V in region I. This is quite similar to the previous analytical solution and considerable unrewarding complication will be avoided by ignoring region III and considering region II to extend as far as necessary. This solution, shown in Figs. 4 and 5, is informative and useful and will

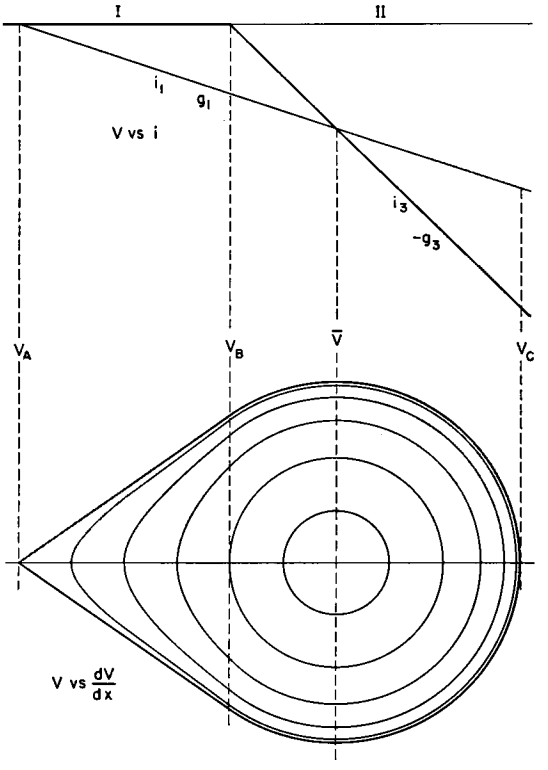

FIGURE 4 *V versus i* characteristics for membrane with negative conductance, $-g_3$, in region II and for series conductance g_1 with axial electrode potential V_A, (upper). Steady state solutions of cable equation on phase plane, *V versus dV/dx* (lower). Outer trajectory is for infinite axon and electrodes and V_C is the potential of center point. Successive inner trajectories are for decreasing axon and electrode lengths. The two inner circles are full wave solutions at the critical length and the center at $\bar{V}$ is solution for shorter lengths.

not differ in any important way from that in which region I is allowed to be slightly conductive or from that for the less idealized characteristic of Fig. 1. From equation (8) the membrane potential V_C at $x = 0$ is

$$V_C = \frac{g_3 + \sqrt{g_1 g_3}}{g_3 - g_1} V_B - \frac{g_1 + \sqrt{g_1 g_3}}{g_3 - g_1} V_A.$$

The dependence of V at other points upon V_A is somewhat more involved but it can be shown directly by elimination of $(V_A - V_B)$ between V and y in equations (7) and (8) that, at each x, $y = m\ (V - V_B)$. The slopes on the phase plane are as shown by the dashed lines in Fig. 6 and m depends only upon g_1, g_2, and g_3 in each region in addition to x. Thus the transition from one steady state solution to another is continuous and relatively simple.

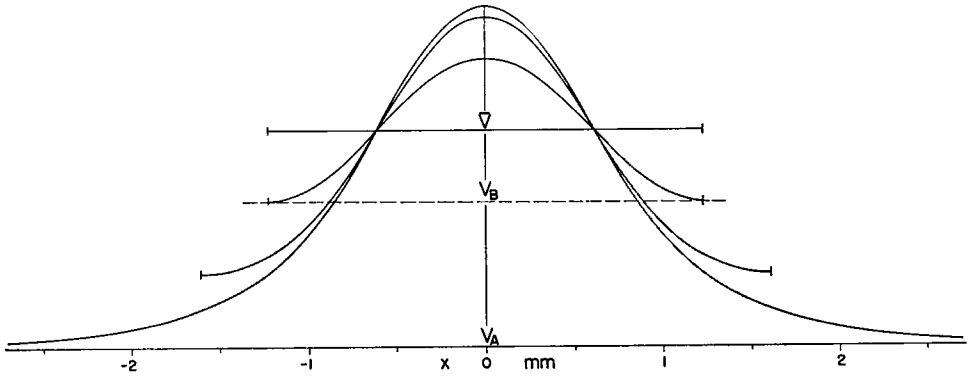

FIGURE 5 Membrane potential V, *versus* distance from center point, x, for axial electrode potential V_A and four of the axon and electrode lengths of Fig. 4. The largest amplitude is for the infinite length, the next is for 3.08 mm, the third is a full wave solution at the critical length, 2.36 mm. The solutions for shorter lengths are constant at $\bar{V}$.

These solutions for an infinite axon are, however, somewhat unsatisfactory in that they contain no condition to require that V_C be at the position chosen for $x = 0$ and either might be anywhere along the axon.

The solution can be fixed in position by the more realistic assumption restricting the electrode region to $-L \leq x \leq L$. The solution with an indefinite length of axon beyond each end of the axial electrode presents some difficulties that have not yet been overcome. It seems necessary to return to the complication of including region III and a satisfactory solution has not been found for $V > V_B$ at the end of the axial electrode. It seems probable that in this situation the real axon starts a propagating impulse to solve its considerably more complicated problem.

The problem is now again made somewhat less practical by assuming non-con-

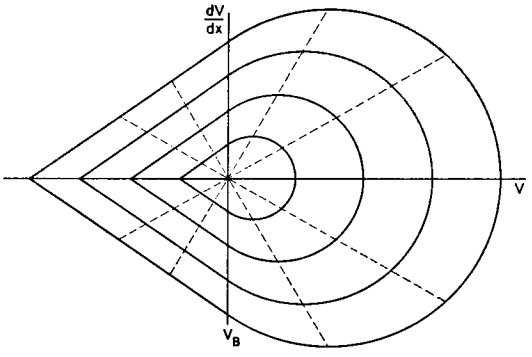

FIGURE 6 Phase plane, V *versus* dV/dx, solutions for infinite axon and electrodes for several values of the axial electrode potential. Each straight line from $(V_B, 0)$ is the path of the solution at one position on the axon as V_A is changed.

ducting boundaries at $x = \pm L$. This might be approached by external vaseline seals and probably well realized by perhaps hazardous external sucrose or internal oil seals. The condition is then $dV/dx = 0$ for $x = \pm L$ and this is fulfilled by the trajectories within the solution given, Figs. 4 and 5, which are hyperbolic for $V < V_B$ and are symmetrical about $x = 0$. As the electrode length is reduced the appropriate trajectory is continuously contracted until it reaches the limiting circle tangent to $V = V_B$. Here the membrane is excited over the entire length, $2L = 2\pi/\omega$. For even shorter lengths no symmetrical solution has been found to satisfy the conditions except the point on the axis where $V = \overline{V}$ and the potential becomes uniform. With the assumed axon and electrode characteristics this critical length

$$2L = 2\pi\sqrt{g_2/(g_3 - g_1)} = 2.36 \text{ mm}.$$

Consequently in such an axon perfect spatial control can only be expected with seals at less than 1.2 mm from the central point although this distance is sufficiently near an axon diameter to suggest an examination of the validity of the approximations used.

Although the minimum wave length is $2L = 2\pi/\omega$, a half wave length also satisfies the boundary condition that $dV/dx = 0$ at both ends and the maximum length of a uniform patch is then $2L = \pi/\omega$ or about 1.2 mm for the axon and electrode characteristics assumed.

As the axon and electrode length is increased with the linear membrane characteristic the half plane trajectory expands abruptly from a point to the peak to valley amplitude of $2(\overline{V} - V_B)$. But if the conductance $-g_3$ in region II gradually becomes less negative nearer regions I or III, as in Fig. 1, the peak to valley amplitude increases continuously for increases of length beyond the critical one.

As the length is increased, with the linear segments for I and II, more of it has the hyperbolic cosine variation of potential until the full wave critical length is reached, when both half and whole plane solutions become possible. Further length increase expands both of these into the hyperbolic cosine region until, at $2L = 3\pi/\omega$, the new, wave length and a half, antisymmetrical, pattern also becomes a possibility. For considerable lengths of terminated axon and electrode everything is then possible from the largest integral number of minimum half wave lengths π/ω, in the total length down to the symmetrical pattern with near exponential ends given by equations (7) and (8) but only this latter solution has been considered further.

An approximate calculation shows that, for large values of L, none of the pertinent quantities x_B, V_C, or V_L depart by more than a few per cent from their values for indefinitely large L when $L = x_B + 3/\alpha$. The nominal values of the axon and electrode properties then give

$$2L = \frac{2}{\omega}\cos^{-1}\left(-\sqrt{g_1/g_3}\right) + 6\sqrt{g_2/(g_1 + g_3)}$$

$$= 1.63 + 3.16 = 4.8 \text{ mm}$$

as an axon and electrode length which will be practically indistinguishable from an axon and electrode of infinite extent but for which V will be a maximum at $x = 0$ and symmetrical about this point.

We will now only consider the solution for the infinite axon and electrode as the convenient and reasonable approximation to a practical arrangement with a length of more than about 5 mm.

STABILITY, ACCURACY, AND SPEED

The solutions thus far obtained have been assumed to be steady states without consideration of their stability. The simplest situation, that of uniform membrane potential and current density over less than the critical axon and electrode length, may be shown to be unstable for $g_3 > g_1$ by qualitative considerations of the effect of small fluctuations (CM). This system is, however, made stable by the feedback correction for such fluctuations. The current, for $V > V_B$ and a membrane capacity, C, is $i = g_1 (V_A - V) = g_3(V_B - V) + C\, dV/dt$ and, introducing the control $V_A = \mu (E - V)$,

$$\frac{C}{(\mu + 1)g_1 - g_3} \cdot \frac{dV}{dt} + V = \frac{\mu g_1 E - g_3 V_B}{(\mu + 1)g_1 - g_3} \tag{10}$$

where μ is the amplification factor of the perfect control amplifier.

Displacements of δE and δV_B produce the steady state change of V

$$\delta V = \frac{\mu g_1}{(\mu + 1)g_1 - g_3}\, \delta E - \frac{g_3}{(\mu + 1)g_1 - g_3}\, \delta V_B$$

while at the time δE and δV_B occur

$$\frac{dV}{dt} = \frac{\mu g_1}{C}\, \delta E - \frac{g_3}{C}\, \delta V_B$$

The potential may be expected to be stable if it changes initially in the direction of its final value and for dV/dt to be of the same sign as δV it is necessary that $\mu > (g_3/g_1) - 1 = 2$. This condition is also found to be sufficient for stability by direct integration of equation (10). The fractional error in the membrane current, i_3, resulting from imperfect potential control is $(g_3 - g_1) / [\mu g_1 - (g_3 - g_1)]$ and the time constant for the control is $C/[\mu g_1 - (g_3 - g_1)]$. These are then usually of the order of $1/\mu$ and $C/\mu g_1$ respectively.

For an axon and electrode of more than critical length it is necessary to return to the spatial conditions,

$$\frac{\partial^2 V}{\partial x^2} = (i_3 - i_1)/g_2$$

$$= \left[g_3(V_B - V) + C \frac{\partial V}{\partial t} - g_1(V_A - V) \right] / g_2$$

or

$$\frac{\partial^2 V}{\partial x^2} - \alpha^2(V - V_A) = \frac{C}{g_2}\cdot\frac{\partial V}{\partial t}, \qquad V_B \geq V \geq V_A \tag{11}$$

$$\frac{\partial^2 V}{\partial x^2} + \omega^2(V - \bar{V}) = \frac{C}{g_2}\cdot\frac{\partial V}{\partial t}, \qquad V \geq V_B \tag{12}$$

It will again be assumed that the axon is bounded but long enough for the steady state solution of equations (7) and (8) to be adequate approximations. The steady state change for displacements δV_A and δV_B is

$$\delta V = -\frac{g_1 + \sqrt{g_1 g_3}\cos\omega x}{g_3 - g_1}\,\delta V_A + \frac{g_3 + \sqrt{g_1 g_3}\cos\omega x}{g_3 - g_1}\,\delta V_B$$

and, initially,

$$\frac{\partial V}{\partial t} = \frac{g_1}{C}\,\delta V_A - \frac{g_3}{C}\,\delta V_B.$$

$\partial V/\partial t$ is thus of opposite sign from δV, for $g_3 > g_1$ and all values of $x \leq x_B$, and this system is expected to be unstable without feedback control. It has not been possible to establish the general validity of this conclusion without a solution of the partial differential equations (11) and (12).

Since the system seems unstable without feedback control, the situation is yet more complicated. Without loss of generality we may place the control point at $x = 0$ so that V_C is the control potential. For $V_A = \mu\,(E - V_C)$ equations (11) and (12) become

$$\frac{\partial^2 V}{\partial x^2} - \alpha^2(V - \mu E) = \frac{C}{g_2}\cdot\frac{\partial V}{\partial t} + \frac{\mu g_1}{g_2}\,V_C(t) \tag{13}$$

$$\frac{\partial^2 V}{\partial x^2} + \omega^2\left(V - \frac{g_3 V_B - \mu g_1 E}{g_3 - g_1}\right) = \frac{C}{g_2}\cdot\frac{\partial V}{\partial t} + \frac{\mu g_1}{g_2}\,V_C(t) \tag{14}$$

In the steady state

$$V = \mu(E - V_C) - [\mu(E - V_C) - V_B]\exp[-\alpha(x - x_B)], \qquad V \leq V_B, \tag{15}$$

$$V = \frac{g_3 V_B - \mu g_1(E - V_C)}{g_3 - g_1} - \frac{\sqrt{g_1 g_3}}{g_3 - g_1}[\mu(E - V_C) - V_B]\cos\omega x, \qquad V \geq V_B. \tag{16}$$

Then

$$V_C = \frac{\mu(g_1 + \sqrt{g_1 g_3})E - (g_3 + \sqrt{g_1 g_3})V_B}{\mu(g_1 + \sqrt{g_1 g_3}) - (g_3 - \bar{g}_1)}$$

and the error

$$E - V_C = \frac{(g_3 + \sqrt{g_1 g_3})V_B - (g_3 - g_1)E}{\mu(g_1 + \sqrt{g_1 g_3}) - (g_3 - g_1)}.$$

The transient solution for equations (13) and (14) has not been found but we may

proceed as before and see whether it starts in the right direction. The final effect of displacements δE and δV_B at the control point is

$$\delta V_C = \frac{\mu(g_1 + \sqrt{g_1 g_3})}{\mu(g_1 + \sqrt{g_1 g_3}) - (g_3 - g_1)} \delta E - \frac{g_3 + \sqrt{g_1 g_3}}{\mu(g_1 + \sqrt{g_1 g_3}) - (g_3 - g_1)} \delta V_B$$

while the initial effect is

$$\frac{\partial V_C}{\partial t} = \frac{\mu g_1}{C} \delta E - \frac{g_3}{C} \delta V_B .$$

For these to be in the same direction it is necessary that $\mu > (g_3 - g_1) / (g_1 + \sqrt{g_1 g_3}) = 0.733$ and it will be assumed that this condition is also sufficient.

At the control point, the fractional error in i_3 is now $(g_3 - g_1)/[\mu (g_1 + \sqrt{g_1 g_3}) - (g_3 - g_1)]$ and the initial time constant is $C(g_1 + \sqrt{g_1 g_3}) / g_1[\mu(g_1 + \sqrt{g_1 g_3}) - (g_3 - g_1)]$. These are again usually of the order of $1/\mu$ and $C/\mu g_1$ respectively.

The most important conclusions are obtained from equations (15) and (16) and it is correspondingly important to find a better basis for expecting them to be stable solutions of equations (13) and (14) as well as more satisfactory to have some understanding of the nature of the transient solution. The only rapid and practical procedure found was the manual numerical integration by conventional methods (Milne, 1953).

First a solution of equations (11) and (12) for the uncontrolled axon was started at a displacement of V_A. The potential moved away from the appropriate steady state and with no indication of return for as long as the integration was continued. Then for the controlled axon of equations (13) and (14) the value of E was decreased by a small amount at $t = 0$ to give the error $\delta V\ (x, 0)$ derived from equations (7) and (8) shown in Fig. 7. For $\mu = (g_3 - g_1)/(g_1 + \sqrt{g_1 g_3}) = 0.733$, $\partial(\delta V)/\partial t$ was zero at all points and the error remained without change. With $\mu = 1$ the error decreased, but too slowly for convenience with the units used, and the integration shown in Fig. 7 was finally carried out with $\mu = 10.5$. The error potential over the whole membrane was first made more negative as the capacity was discharged with a time constant of approximately $C/\mu g_1$. As the error at the control point came to zero, the more remote points began to return towards the steady state and were later assisted to do so by a slightly negative control point error as all potentials moved more and more slowly toward the new steady state distribution. On the phase plane, the original steady state trajectory was initially translated almost unchanged to lower potentials until V_C was near its new value and then the rest of the trajectory expanded to its new steady state. In this process the axial wire potential changed by 10.5 times the control point error at all times.

This integration shows that the transient process is rather complicated and although the control point moves towards its new value with considerable speed, other points not far away will take on larger errors which are only corrected quite slowly. More importantly, the integration gives additional reason to believe that for present

purposes the steady state solutions such as equations (15) and (16) are indeed stable and with but little control.

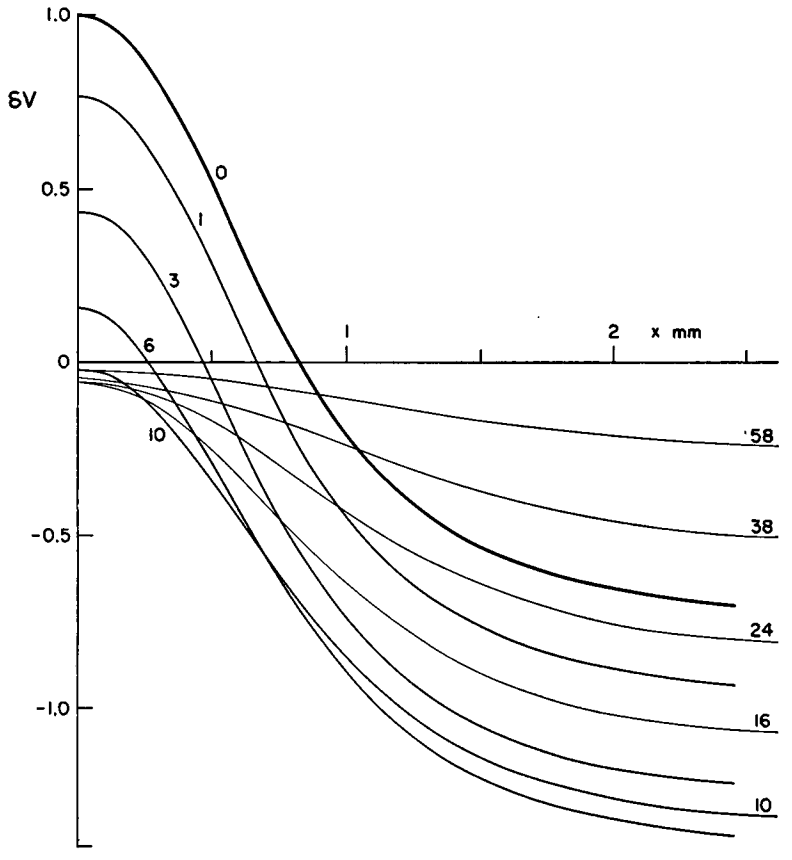

FIGURE 7 Numerical solutions of equations (13) and (14) for the change of membrane potential, δV, ordinates, *versus* distance at indicated times after a change of the control command, δE. The distribution at $t = 0$ is the difference between the initial and final steady states. The intermediate times are in units of 0.141 μ sec., the control amplification, μ, is 10.5, and the control point is at $x = 0$. The control point is brought rapidly to near its final value and the more distant points are corrected more slowly.

COMMENTS AND CONCLUSIONS

This analysis had been confined to the point control system in part because it has not appeared particularly easy to formulate the problem for extended potential electrodes, but largely for other practical reasons. The present experimental evidence leads to the conclusion that with a potential control near the axis of a good axon the added axoplasm resistance might be too much for stability, and certainly

would be for accuracy. In addition to their unreliability the extended internal potential electrodes that have been used have not been placed close enough to the membrane to give some promise of stability and accuracy with even a rather uniform axon (CM).

The entire analysis has been based on the assumption that the membrane potential is constant around any circumference of the axon. As has been pointed out (CM) such results should not be accepted without reservation when significant distances along the axon are comparable to its diameter. Furthermore it should be remembered from CM and TMC that there is still some experimental uncertainty in the values of the electrode resistances and those of the axoplasm and sea water between them and the potential electrodes and also for the resistance between the potential electrodes and the capacity and conductance of the membrane.

The electrode and electrolyte characteristics that have been assumed give not the worst possible situation but one that is not far from it. As the electrode and electrolyte conductance, g_1, becomes so small as to be negligible, the frequency parameter, ω, only increases from 2.7 mm^{-1} to 3.2 mm^{-1}. Conversely, as this conductance and the negative membrane conductance approach each other numerically, ω decreases to broaden the current density pattern as it approaches uniformity and stability. With the practically perfect electrodes used recently the clamp is stable and the potential uniform for more of the better axons including those with negative membrane resistances down to -4 ohm cm^2. Nonetheless the axoplasm and sea water still produce an ω of 2.3 mm^{-1} for the nearly best of the axons so far encountered.

The assumptions used are also quite conservative in another respect as shown by Chandler (1961). The linear negative membrane conductance $-g_3$ has been taken throughout region II as that of maximum slope in this region. The membrane is thus expected to be inherently stable at potentials and distances that are somewhat less removed from those of the maximum instability that have been given here. Consequently the experimental requirements ought not to exceed the predictions in this respect at least.

An unexpected development is the appearance of a uniform potential over a sufficiently short length of axon. This behavior is similar and perhaps closely analogous to that of a longitudinally compressed column fixed at both ends. The column is completely stable for a particular load up to a critical length but beyond this length it will buckle. It may well be that such a solution has already been presented by the single node and somewhat spherical cells, and something similar can be expected as a necessary condition for successful clamping with virtual internal potential electrodes.

The complex of possibilities for longer axon and electrode lengths might explain the considerable variety of potential and current distributions that have appeared (TMC), but there is probably a stability condition to determine which of all these patterns will remain after transients have died out. There are also many assump-

tions and approximations between these possibilities and reality while the two patch experiments (TMC) further suggest that non-uniformity is of particular importance. But there is also the principle of parsimony and on the strength of it we have confined our attention to the already tedious solution given by equations (7) and (8).

With a finite length of axon and electrodes the maximum of potential for this solution is at the center. If the control is not at this point it is to be expected that V_A will decrease and the entire pattern will enlarge to bring the control point appropriately close to the command. These situations have not been investigated but it is seen that in spite of a high gradient, the average potential over a short length might actually be more adequate than for the control point at the center.

A definite shortcoming at the present work is the lack of an analytical expression for the transient characteristics or a general criterion of stability for the problem and without these any intuitive and numerical approaches are of limited value. There are as yet no apparent hazards in the immediate vicinity of the calculations made and since these are on the dangerous side of the axon characteristics to be expected, it is felt that the predictions are conservative.

Two factors that had certainly been no more than vaguely realized in the course of a considerable experimental experience are the almost insignificant control amplification requirements for stability at the control point and the extreme rapidity of error corrections at that point with perfect amplification. Although some of the implications seem rather obvious, the extent to which these observations may be found a useful guide to equipment and experiment design and operation is far from certain!

It seems reasonable to conclude:

that the membrane potential can be well controlled at the control point;

that, with the present experimental arrangement, instability and a consequent considerable variation of membrane potential are to be expected away from this point;

but that under even rather conservative assumptions reasonably accurate current measurements can be made within a few tenths of a millimeter of the control point.

The suggestions, criticisms, and assistance of Dr. W. K. Chandler, Dr. R. E. Taylor, Dr. J. M. Moore, and particularly of Dr. R. FitzHugh have been helpful throughout this work and are gratefully acknowledged.

Received for publication, December 28, 1960.

REFERENCES

CHANDLER, W. K., 1961, Biophysical Society Abstracts, St. Louis, Mo., FC4.
COLE, K. S., *Arch. sc. physiol.*, 1949, **3**, 253.
COLE, K. S., and MOORE, J. W., (CM) *J. Gen. Physiol.*, 1960, **44**, 123.

HODGKIN, A. L., HUXLEY, A. F., and KATZ, B., (HHK) *J. Physiol.*, 1952, **116,** 424.
HODGKIN, A. L., and HUXLEY, A. F., (HH) *J. Physiol.*, 1952*a*, **116,** 449.
HODGKIN, A. L., and HUXLEY, A. F., (HH) *J. Physiol.*, 1952*b*, **116,** 473.
HODGKIN, A. L., and HUXLEY, A. F., (HH) *J. Physiol.*, 1952*c*, **116,** 497.
HODGKIN, A. L., and HUXLEY, A. F., (HH) *J. Physiol.*, 1952*d*, **117,** 500.
MILNE, W. E., Numerical Solution of Differential Equations, New York, John Wiley and Sons, Inc., 1953.
MINORSKY, N., Introduction to Non-linear Mechanics, J. W. Edwards, Ann Arbor, Michigan, 1947.
TAYLOR, R. E., MOORE, J. W., and COLE, K. S., (TMC) *Biophysic. J.*, 1960, **1,** 161.